

Supporting Information for

Towards large tubular helices based on the polymerization of tri(benzamide)s

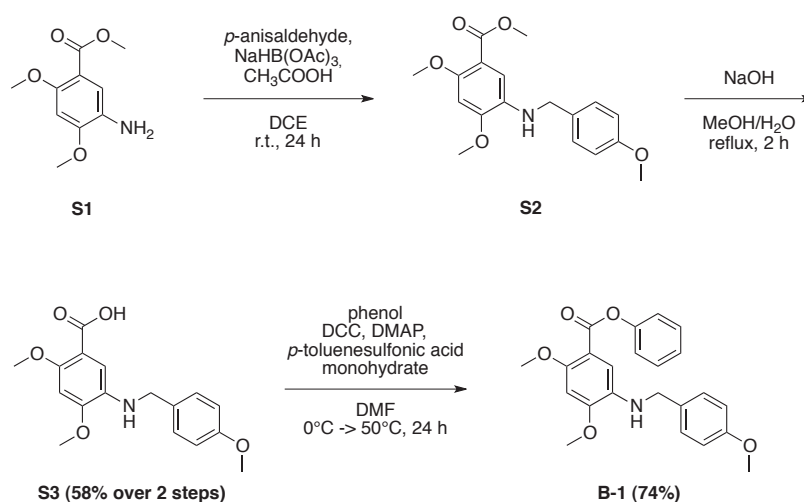
Maren Schulze, Andreas F.M. Kilbinger

University of Fribourg, Department of Chemistry, Chemin du Musée 9, CH-1700 Fribourg, Switzerland

Correspondence to: Andreas F.M. Kilbinger (E-mail: andreas.kilbinger@unifr.ch)

Experimental

Synthesis of phenyl 2,4-dimethoxy-5-((4-methoxybenzyl)amino)benzoate (B-1)



Scheme S1. Synthetic route to the bent monomer **B-1**.

Methyl-2,4-dimethoxy-5-aminobenzoate (S1)

Methyl-2,4-dimethoxy-5-nitrobenzoate¹ (5.00 g, 0.021 mol) and ammonium formate (13.07 g, 0.210 mol) were dissolved in methanol (150 mL) and dimethylformamide (15 mL). Palladium on activated charcoal (10%, 0.48 g) was slowly added under a gentle flow of argon gas while stirring the suspension at 0°C. The mixture was stirred at room temperature overnight. To remove the catalyst, the solution was filtered over celite and the filtrate was evaporated under vacuum. The residual solution was dissolved in water and extracted with ethyl acetate. The combined organic layers were dried over magnesium sulfate and the solvent removed under reduced pressure. The brown oil was dried at the Schlenk line to give **S1** (4.36 g, 0.0206 mol, 98%) as grey crystals. ¹H NMR (360 MHz, CDCl₃): δ (ppm) = 3.71 (s, 3 H, OCH₃), 3.75 (s, 3 H, OCH₃), 3.85 (s, 3 H, OCH₃), 4.55 (s, 2 H, NH₂), 6.61 (s, 1 H, Ar-H³), 7.08 (s, 1 H, Ar-H⁶); ¹³C NMR (90 MHz, CDCl₃): δ (ppm) = 51.52, 55.45, 57.06, 96.95, 111.17, 117.47, 129.19, 151.57, 154.07, 166.14; HR-MS (ESI⁺): *m/z* calculated for [C₁₀H₁₄NO₄]⁺ = 212.09228, found 212.09165; RP-HPLC: 4.90 min.

¹ Zhu, J.; Parra, R. D.; Zeng, H.; Skrzypczak-Jankun, E.; Zeng, X. C.; Gong, B., *J. Am. Chem. Soc.* **2000**, *122*, 4219-4220.

Methyl 2,4-dimethoxy-5-((4-methoxybenzyl)amino)benzoate (S2)

Methyl-2,4-dimethoxy-5-aminobenzoate **S1** (3.50 g, 16.6 mmol) and *p*-anisaldehyde (2.71 g, 19.9 mmol) were dissolved in dichloroethane (80 mL) and glacial acetic acid (4.75 mL, 83 mmol) was added. The mixture was stirred at room temperature for 30 minutes, after which sodium triacetoxyborohydride (7.04 g, 33.2 mmol) was added. The reaction was stirred for 24 h and then quenched with saturated sodium hydrogencarbonate. The aqueous layer was extracted four times with dichloromethane, the combined organic layers were washed with brine, dried over magnesium sulfate and the solvent was removed under reduced pressure to yield methyl 2,4-dimethoxy-5-((4-methoxybenzyl)amino)-benzoate as orange oil which was used in the next step without further purification. ¹H NMR (300 MHz, CDCl₃): δ (ppm) = 3.81 (s, 3 H, OCH₃), 3.86 (s, 3 H, OCH₃), 3.87 (s, 3 H, OCH₃), 3.88 (s, 3 H, OCH₃), 4.25 (s, 2 H, CH₂), 4.62 (s, 1 H), 6.49 (s, 1 H, Ar-H³), 6.89 (d, ³J = 8.69 Hz, 2 H, DMB-H^{3, 5}), 7.18 (s, 1 H, Ar-H⁶), 7.31 (d, ³J = 8.88 Hz, 2 H, DMB-H^{2, 6}); HR-MS (ESI⁺): *m/z* calculated for [C₁₈H₂₂NO₅]⁺ = 332.14980, found 332.14905; RP-HPLC: 10.97 min.

2,4-Dimethoxy-5-((4-methoxybenzyl)amino)benzoic acid (S3)

Methyl 2,4-dimethoxy-5-((4-methoxybenzyl)amino)benzoate **S2** (16.6 mmol) and sodium hydroxide (1.33 g, 33 mmol) were dispersed in a 1:1-mixture of methanol and water (150 mL) and heated under reflux for 2 h. Methanol was removed under reduced pressure, the aqueous phase acidified to pH 3 with 3 N hydrochloric acid and extracted four times with ethyl acetate to give 2,4-dimethoxy-5-((4-methoxybenzyl)amino)benzoic acid (3.07 g, 9.7 mmol, 58% over 2 steps) as a beige powder. ¹H NMR (300 MHz, CDCl₃): δ (ppm) = 3.80 (s, 3 H, OCH₃), 3.91 (s, 3 H, OCH₃), 4.01 (s, 3 H, OCH₃), 4.26 (s, 2 H, CH₂), 6.49 (s, 1 H, Ar-H³), 6.88 (d, ³J = 8.59 Hz, 2 H, DMB-H^{3, 5}), 7.30 (s, ³J = 8.59 Hz, 2 H, DMB-H^{2, 6}), 7.37 (s, 1 H, Ar-H⁶); ¹³C NMR and APT (75 MHz, CDCl₃): δ (ppm) = 47.68 (+), 55.23 (-), 55.79 (-), 57.44 (-), 95.13 (-), 109.51 (+), 112.49 (-), 113.96 (-), 129.06 (-), 130.84 (+), 133.41 (+), 151.26 (+), 151.94 (+), 158.87 (+), 165.83 (+); HR-MS (ESI⁺): *m/z* calculated for [C₁₇H₂₀NO₅]⁺ = 318.13415, found 318.13374; RP-HPLC: 9.62 min.

Phenyl 2,4-dimethoxy-5-((4-methoxybenzyl)amino)benzoate (B-1)

A solution of 2,4-dimethoxy-5-((4-methoxybenzyl)amino)benzoic acid **S3** (3.03 g, 9.5 mmol) in dry DMF (15 mL) was cooled to 0°C and phenol (1.08 g, 11.4 mmol), DMAP (1.45 g, 11.9 mmol) and *p*-toluenesulfonic acid monohydrate (1.81 g, 9.5 mmol) in dry DMF (15 mL) were added dropwise. DCC (2.61 g, 12.6 mmol) in dry DMF (45 mL) was subsequently added dropwise and stirred at 50°C for 24 h. Diethyl ether was added to the mixture, the solid was filtered and water was added. The aqueous phase was extracted with diethyl ether and the combined organic layers were washed with saturated sodium hydrogencarbonate solution, dried over magnesium sulfate and the solvent was removed under reduced pressure. 2 g of the crystalline solid (4.64 g) were purified by column chromatography with hexanes/ethyl acetate (1:1) as eluent to give the bent monomer **B-1** (1.2 g, 3.1 mmol) as yellowish crystals in 74% yield. *R*_f = 0.53. ¹H NMR (300 MHz, CDCl₃): δ (ppm) = 3.81 (s, 3 H, OCH₃), 3.92 (s, 6 H, OCH₃), 4.30 (s, 2 H, CH₂), 6.55 (s, 1 H, Ar-H³), 6.91 (d, ³J = 8.50 Hz, 2 H, DMB-H^{3, 5}), 7.21–7.23 (m, 3 H, DMB-H^{2, 6}, Ph), 7.33–7.44 (m, 5 H, Ar-H⁶, Ph); ¹³C NMR and DEPT (75 MHz, CDCl₃): δ (ppm) = 47.99 (-), 55.21 (+), 55.60 (+), 57.62 (+), 97.28 (+), 110.60 (+), 112.62 (+), 113.93 (+), 121.97 (+), 125.34 (+), 129.07 (+), 129.18 (+), 131.14, 132.19, 151.17, 151.93, 154.27, 158.84, 164.24; HR-MS (ESI⁺): *m/z* calculated for [C₂₃H₂₄NO₅]⁺ = 394.16545, found 394.16551; RP-HPLC: 15.69 min.

Formation of a cyclic trimer from trimer T-1

Discussion

In a further attempt to polymerize **T-1**, we increased the monomer concentration, as cycle formations are typically favored in diluted solutions.² Thus, we polymerized trimer **T-1** directly by addition of 2.2 eq. LiHMDS (1M in THF) with a resulting monomer concentration of 0.44 mol/L. GPC (chloroform) and MALDI-ToF MS measurements proved that the cyclic trimer was again obtained as the major product. The MALDI-ToF spectrum also showed the formation of the cyclic hexamer (with very low intensity). However, the

² Rossa, L.; Vogtle, F., *Top. Curr. Chem.* **1983**, *113*, 1-86.

changes in the GPC-elugram and the MALDI-ToF mass spectrum of the second polymerization were not significant. In summary, both polycondensation attempts of trimeric monomer **T-1** led predominantly to the formation of the cyclic trimer at both concentrations investigated.

The reason for this favored cycle formation is most likely a preference for a conformation that favors the intramolecular ring closing reaction. Such "directed macrocyclization reactions" have previously been described by Carver et al.³ and more recently by us.⁴ Campbell et al. also observed a macrocyclization of an *N*-substituted tri(*p*-benzamide).⁵ The crystal structure of an *N*-alkylated tri(*p*-benzamide) reported by Tanatani et al.⁶ furthermore supports the calculations of the energy-minimized conformation.

The Yokozawa group also observed cyclization as a side reaction during polycondensation of PMB-substituted monomers. They polymerized differently 4-alkyloxy-substituted, *N*-protected phenyl 3-aminobenzoates in a chain-growth polycondensation reaction.⁷ There, the formation of cyclic trimers was proportional to the quantity of self-condensation observed. In their case, cycles could also be synthesized selectively by a slow addition of LiHMDS without the use of initiator yielding 70% of pure cyclic trimer after purification. On the other hand, the chain-growth polycondensation of unsubstituted, *N*-alkylated and *N*-protected phenyl 3-aminobenzoates led exclusively to polymers.⁸ It was proposed that the *ortho*-alkylation (in reference to the protected amine) results in a decrease of the amine proton-acidity through intramolecular hydrogen bond formation. A slow abstraction of the proton would then cause self-condensation in an otherwise initiated polycondensation between deprotonated and non-deprotonated monomers due to their higher concentration in solution. Consequently, macrocyclization reactions are promoted by a combination of the conformational flexibility of the *N*-protected monomers and the introduction of an *ortho*-substituent. However, several questions with regard to the exclusive generation of polymers remain open. The influence of the temperature, the monomer concentration and the choice of solvent on the cyclization process will be thoroughly investigated in the future.

³ Carver, F. J.; Hunter, C. A.; Shannon, R. J., *Chem. Commun.* **1994**, 1277-1280.

⁴ Storz, C.; Hauke, C.M.; Kühnle, A.; Kilbinger, A.F.M. *J. Am. Chem. Soc.* **2014**, *136*, 12832

⁵ Campbell, F.; Plante, J.; Carruthers, C.; Hardie, M. J.; Prior, T. J.; Wilson, A. J., *Chem. Commun.* **2007**, 2240-2242.

⁶ Tanatani, A.; Yokoyama, A.; Azumaya, I.; Takakura, Y.; Mitsui, C.; Shiro, M.; Uchiyama, M.; Muranaka, A.; Kobayashi, N.; Yokozawa, T., *J. Am. Chem. Soc.* **2005**, *127*, 8553-8561.

⁷ Ohishi, T.; Suzuki, T.; Niiyama, T.; Mikami, K.; Yokoyama, A.; Katagiri, K.; Azumaya, I.; Yokozawa, T., *Tetrahedron Lett.* **2011**, *52*, 7067-7070.

⁸ (a) Ohishi, T.; Sugi, R.; Yokoyama, A.; Yokozawa, T., *J. Polym. Sci., Part A: Polym. Chem.* **2006**, *44*, 4990-5003; (b) Sugi, R.; Yokoyama, A.; Furuyama, T.; Uchiyama, M.; Yokozawa, T., *J. Am. Chem. Soc.* **2005**, *127*, 10172-10173.

Analytical-Data

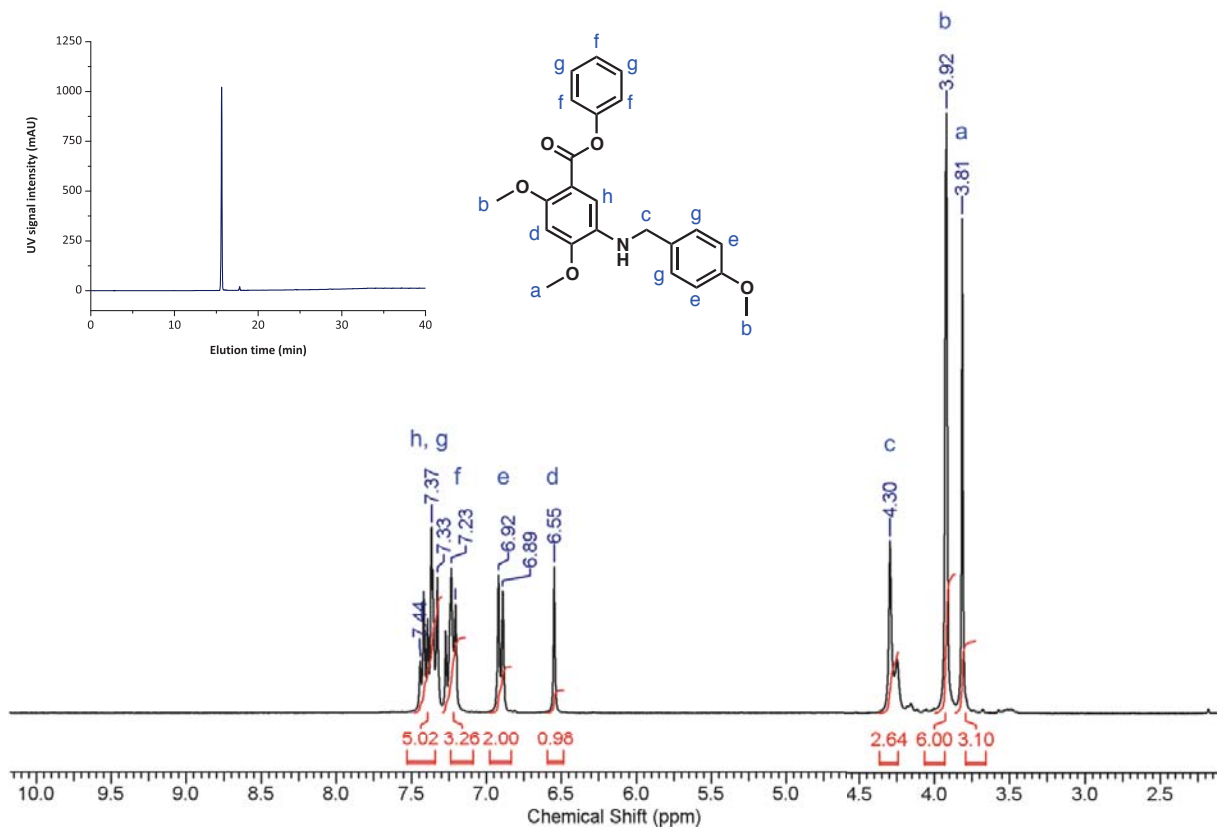


Figure S1. ^1H NMR spectrum (300 MHz, CDCl_3) and RP-HPLC elugram (*inset*) of bent monomer **B-1**.

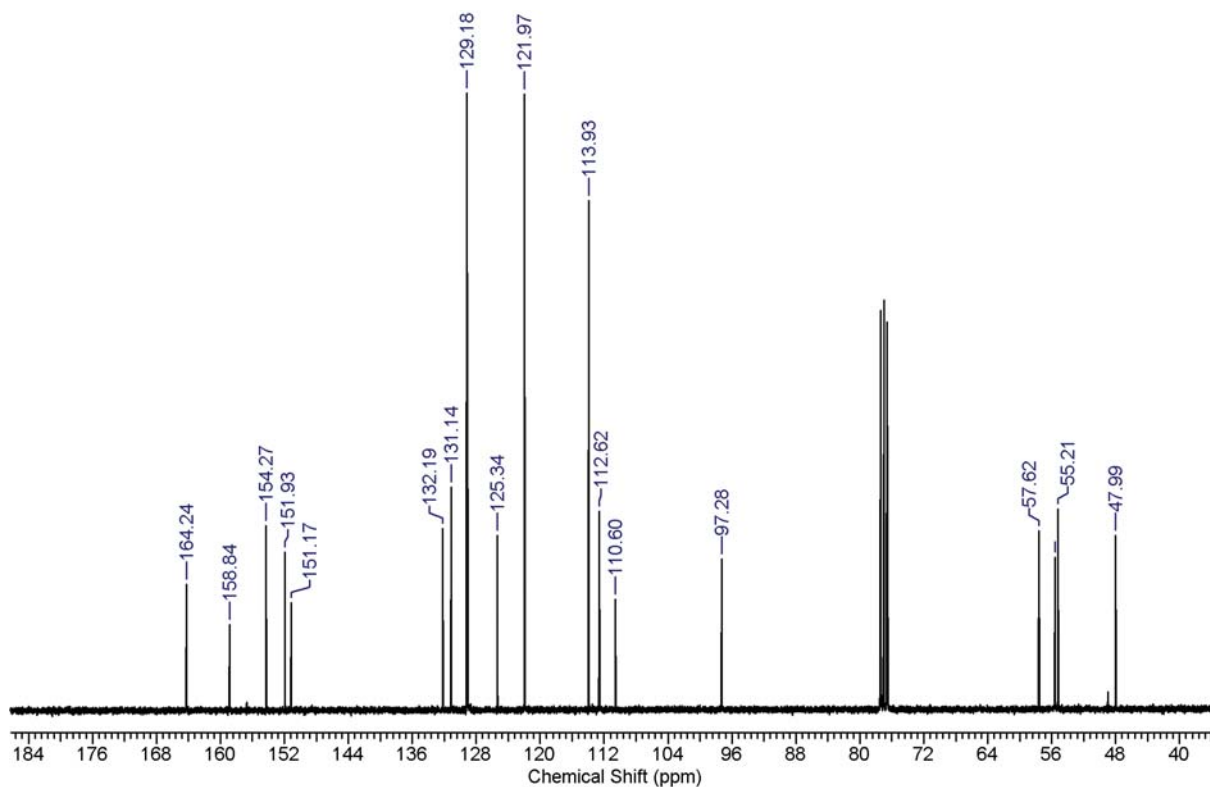


Figure S2. ^{13}C NMR spectrum (75 MHz, CDCl_3) of **B-1**.

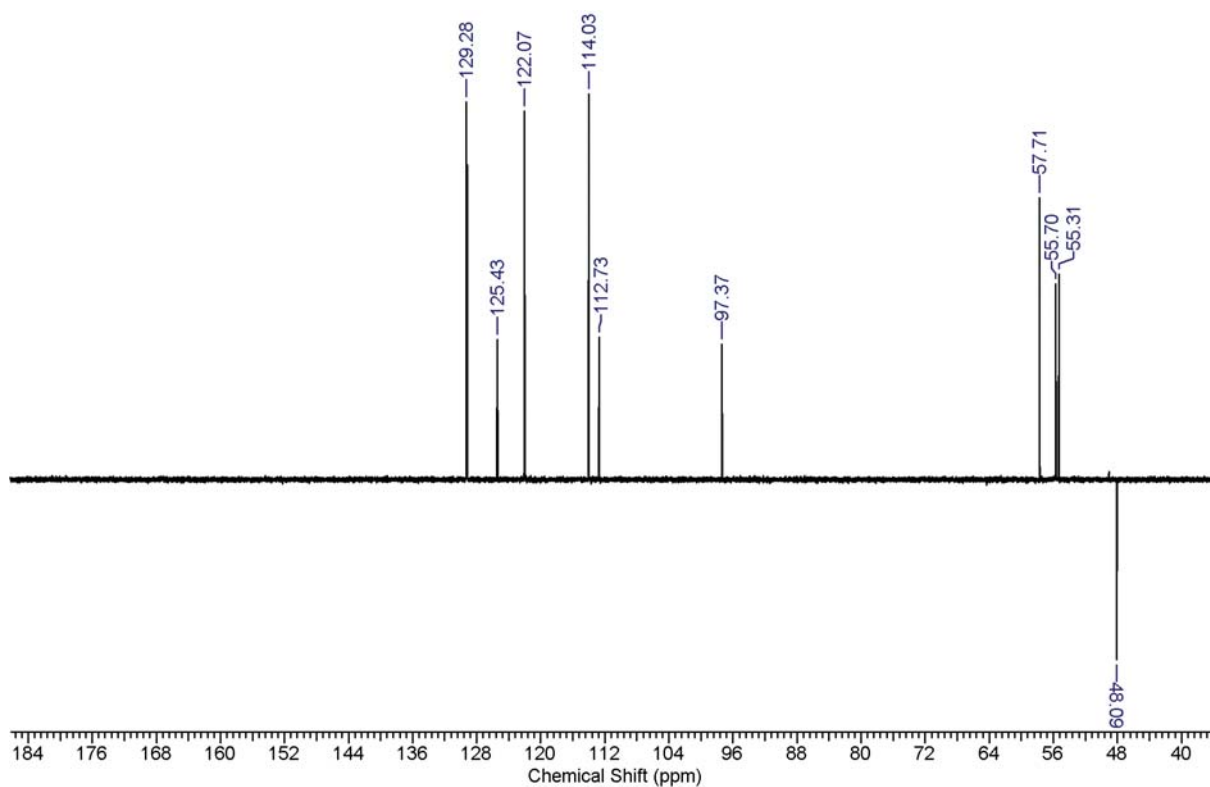


Figure S3. DEPT spectrum (75 MHz, CDCl₃) of B-1.

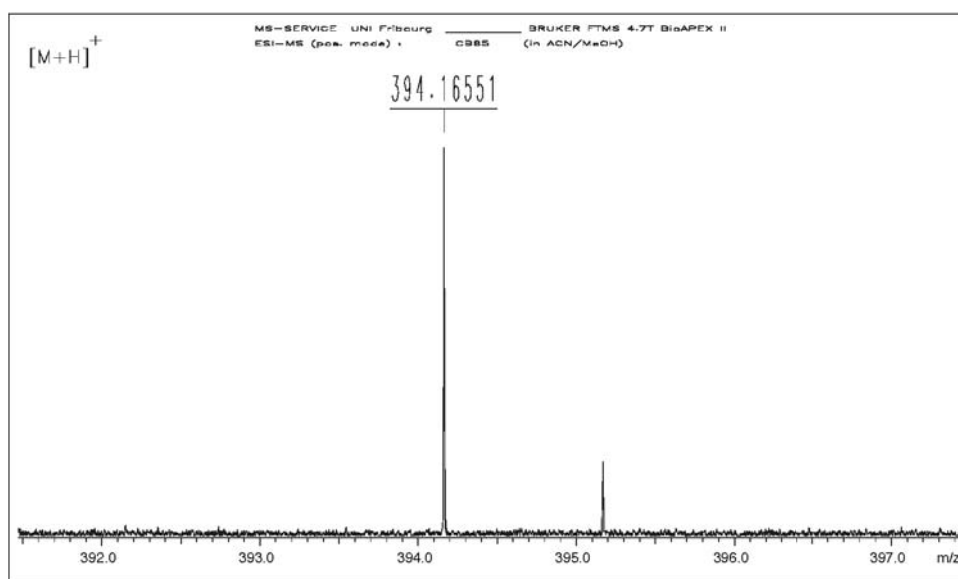


Figure S4. High-resolution mass spectrum (ESI+) of B-1 ([C₂₃H₂₄NO₅]⁺ calc. = 394.16545).

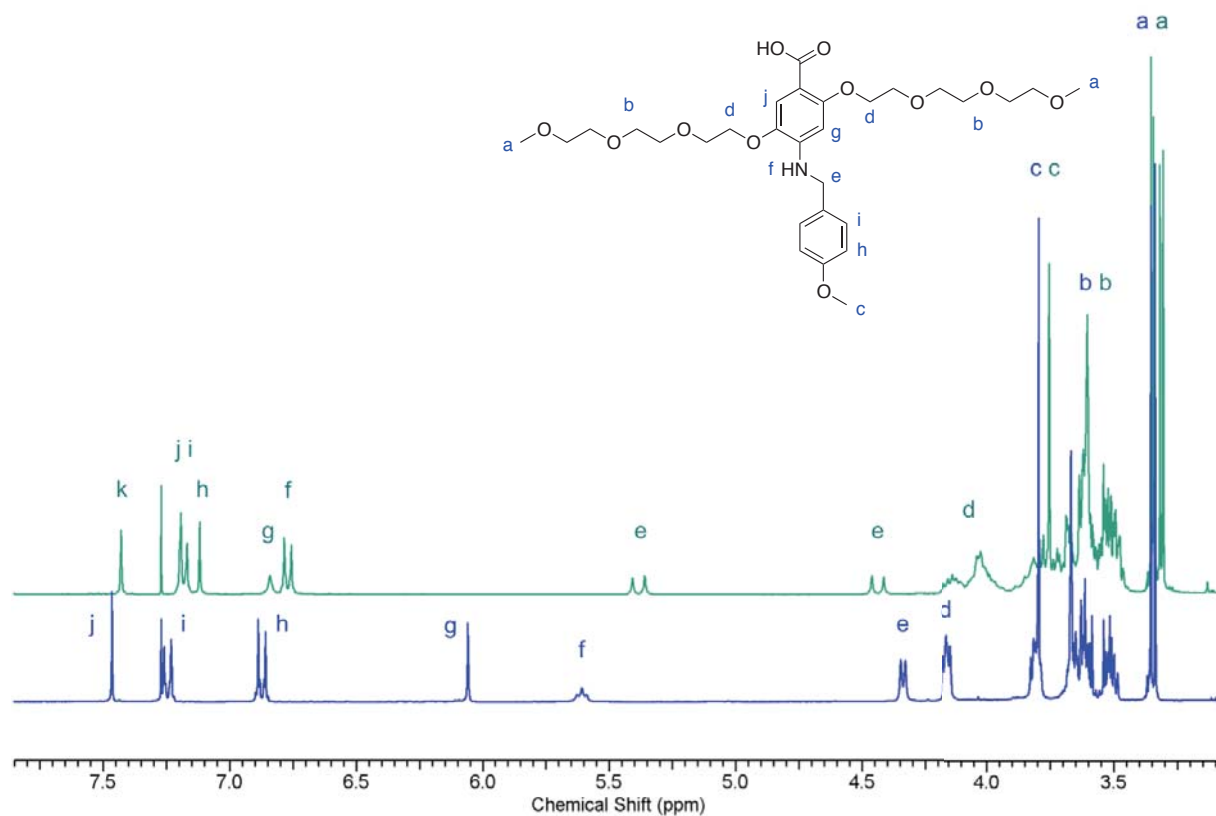


Figure S5. Comparison of the ^1H NMR spectra (300 MHz, CDCl_3) of monomer **L-2** (blue) and dimer **2** (green).

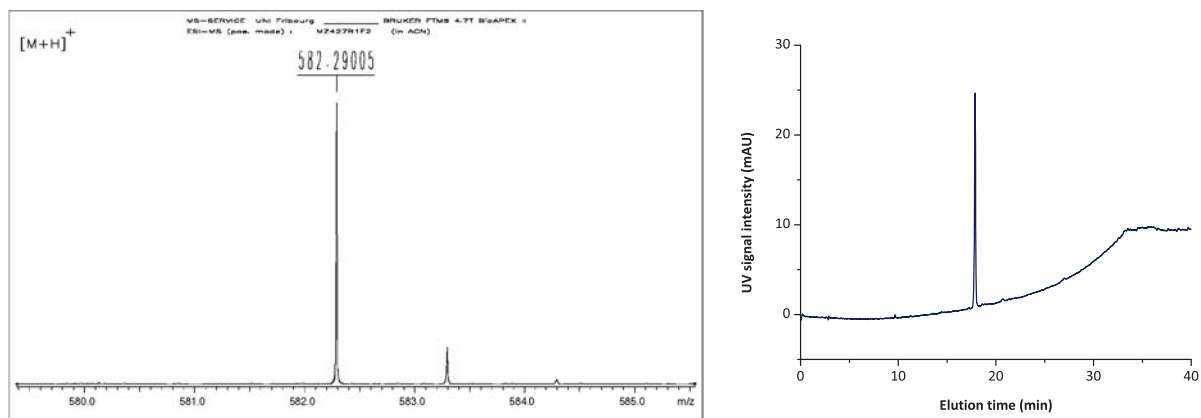


Figure S6. High-resolution mass spectrum (ESI+, $[\text{C}_{29}\text{H}_{44}\text{NO}_{11}]^+$ $\text{calc.} = 582.29144$, left) and RP-HPLC elugram (right) of the PMB-protected monomer **L-2** after purification by recycling HPLC.

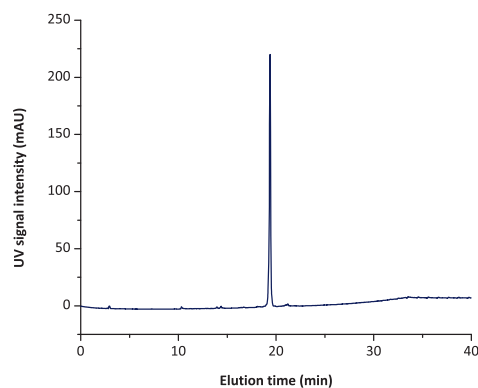
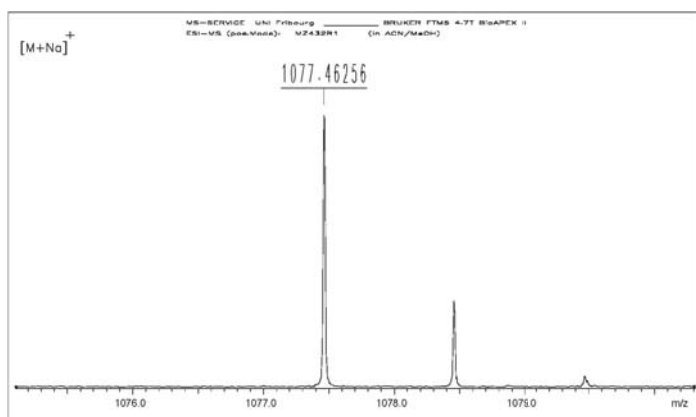


Figure S7. High-resolution mass spectrum (ESI+, $[C_{50}H_{74}N_2O_{22}Na]^+_{\text{calc.}} = 1077.46310$, *left*) and RP-HPLC elugram (*right*) of dimer **2** after purification by recycling HPLC.

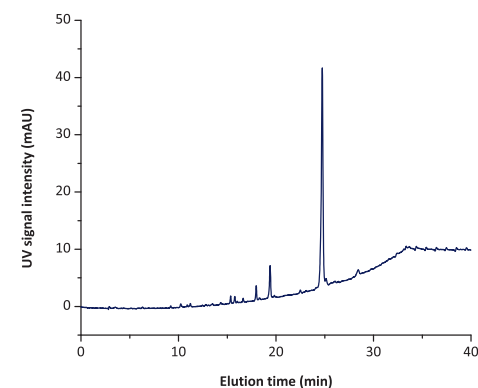
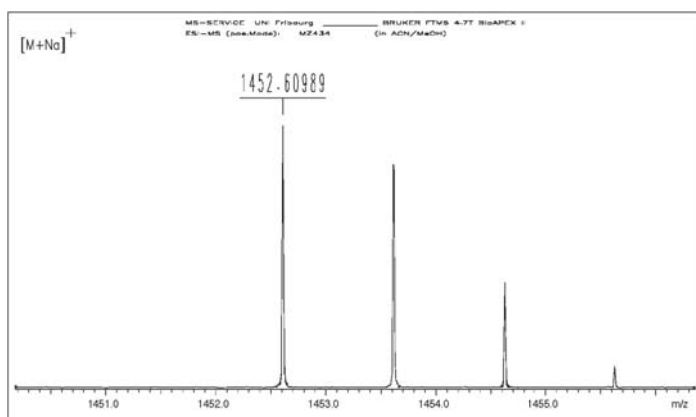


Figure S8. High-resolution mass spectrum (ESI+, $[C_{73}H_{95}N_3O_{26}Na]^+_{\text{calc.}} = 1452.61016$, *left*) and RP-HPLC elugram (*right*) of trimer **3**.

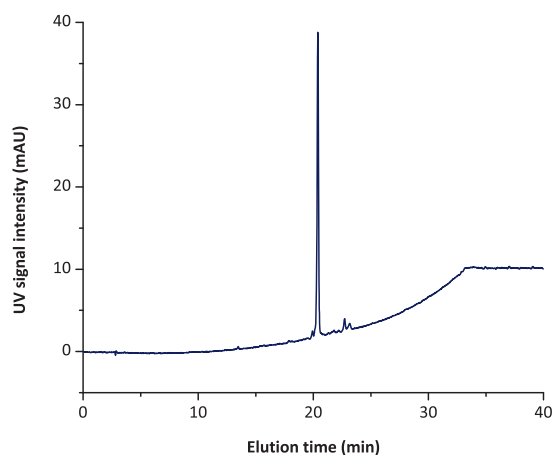
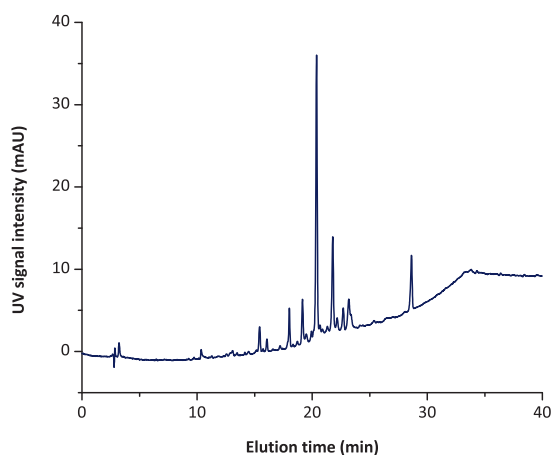


Figure S9. RP-HPLC elugrams of trimer **T-1** before (*left*) and after purification by recycling HPLC (*right*).

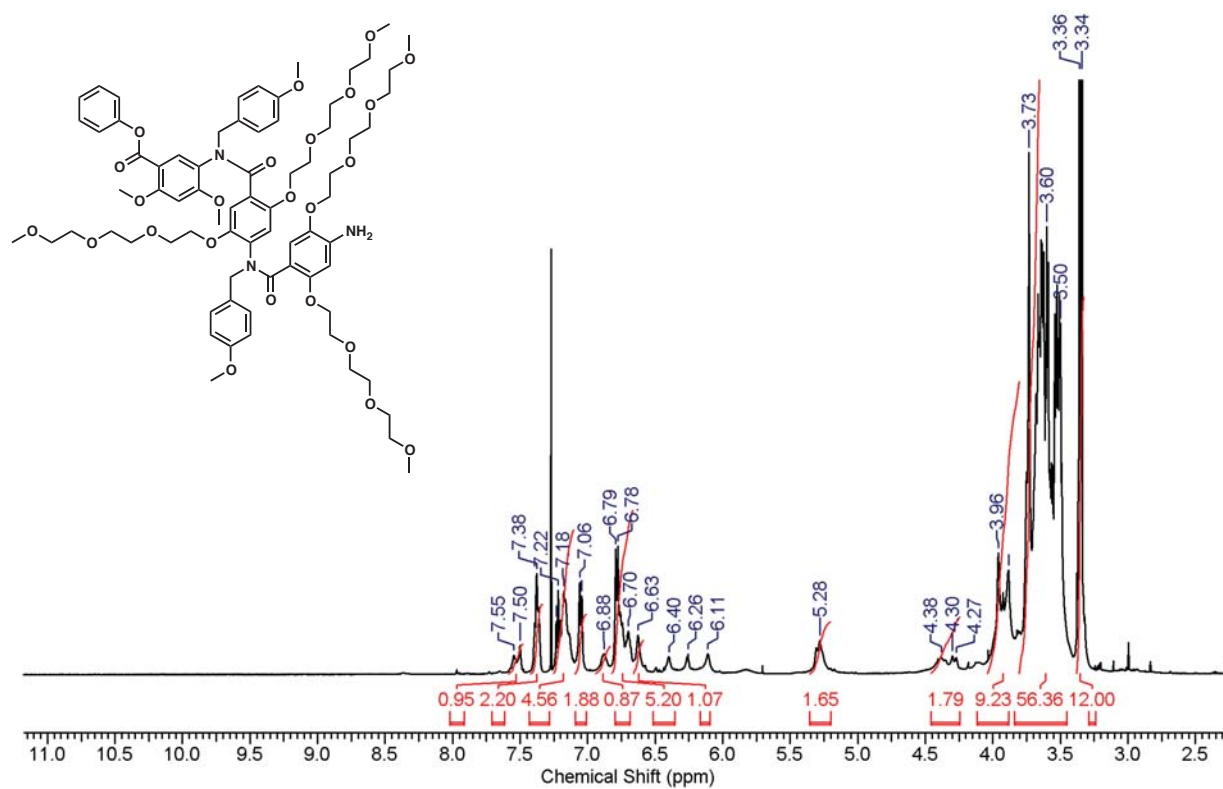


Figure S10. ¹H NMR spectrum (500 MHz, 52°C, CDCl₃) of trimer T-1.

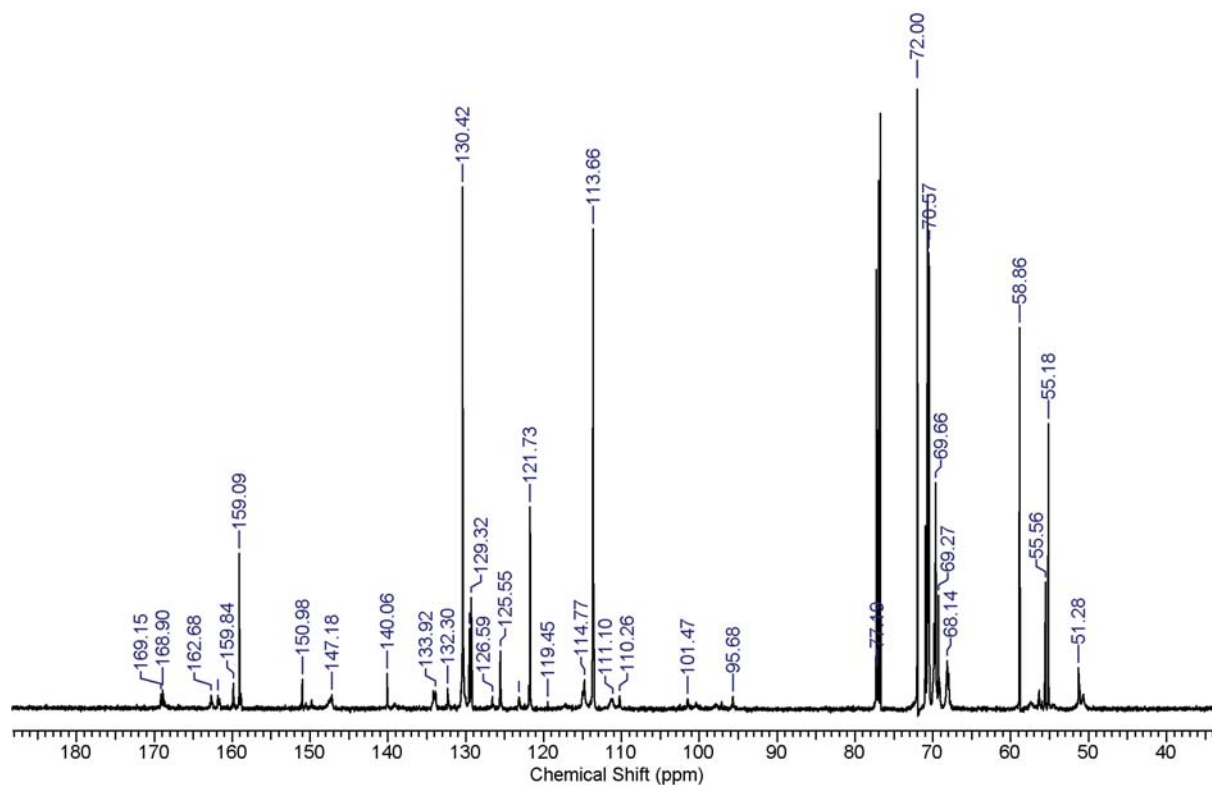


Figure S11. ¹³C NMR spectrum (125 MHz, 52°C, CDCl₃) of trimer T-1.

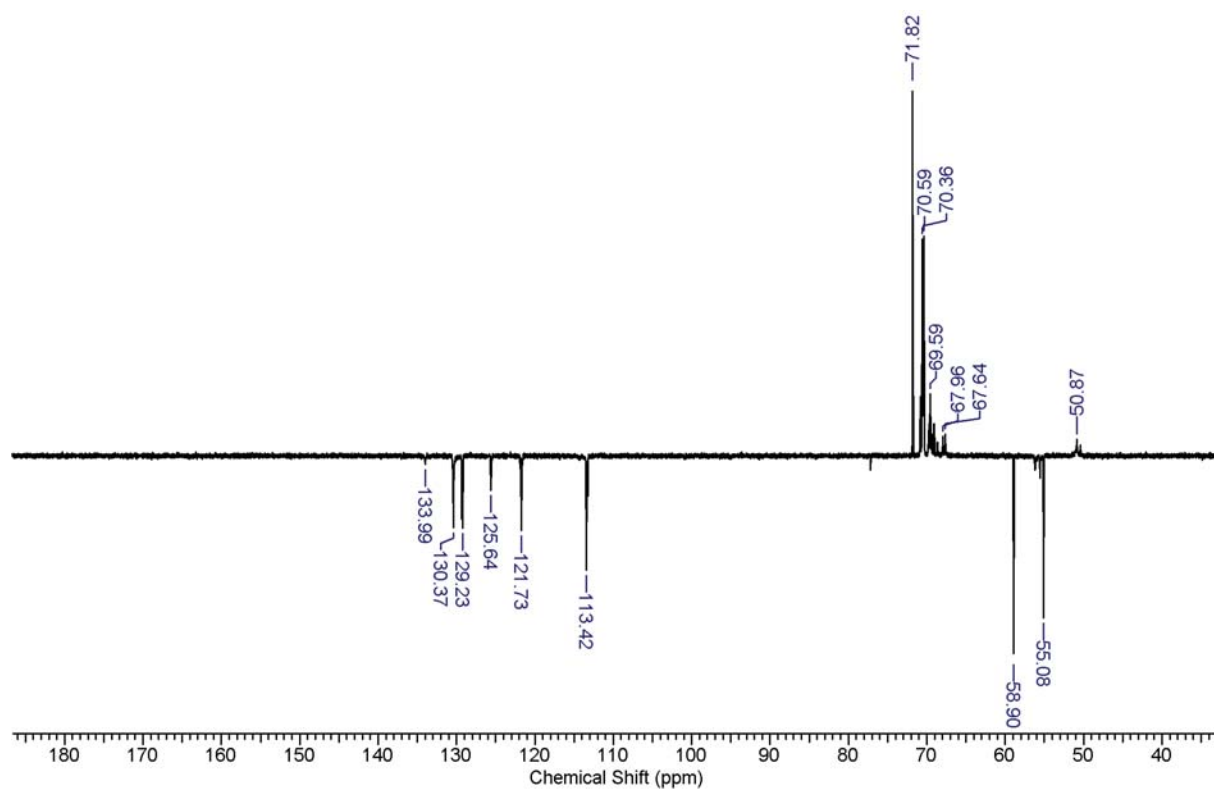


Figure S12. DEPT spectrum (125 MHz, CDCl_3) of trimer T-1.

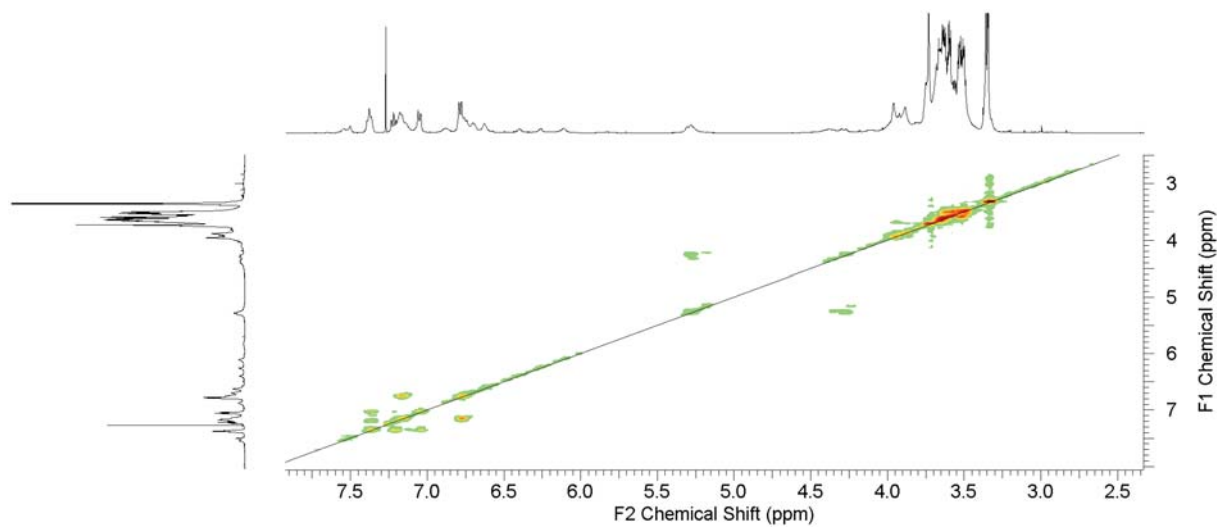


Figure S13. COSY spectrum (500 MHz, 52°C, CDCl_3) of trimer T-1.

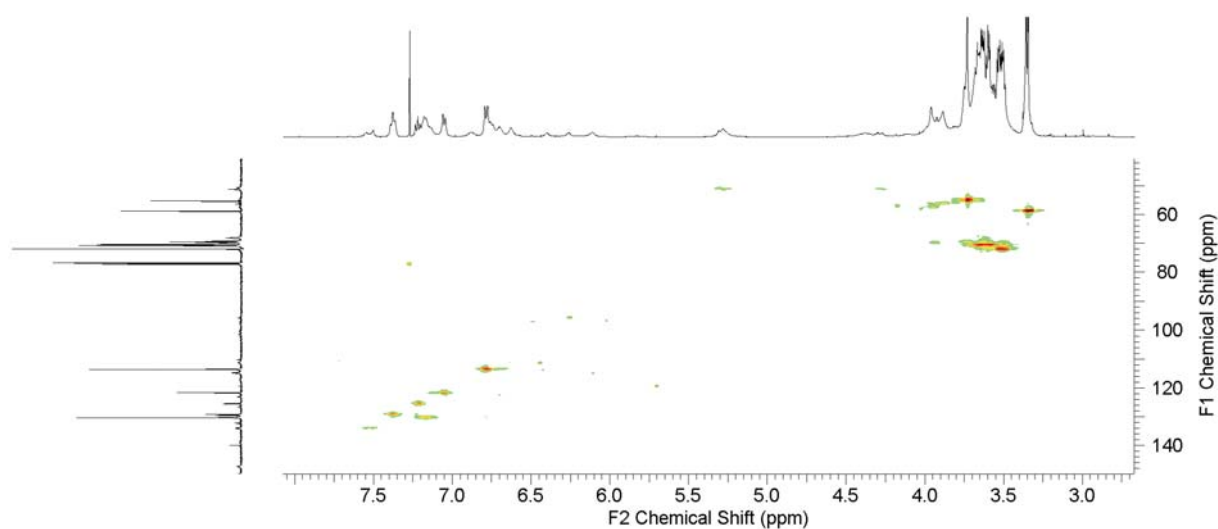


Figure S14. HMQC spectrum (500 MHz, 125 MHz, 52°C, CDCl₃) of trimer **T-1**.

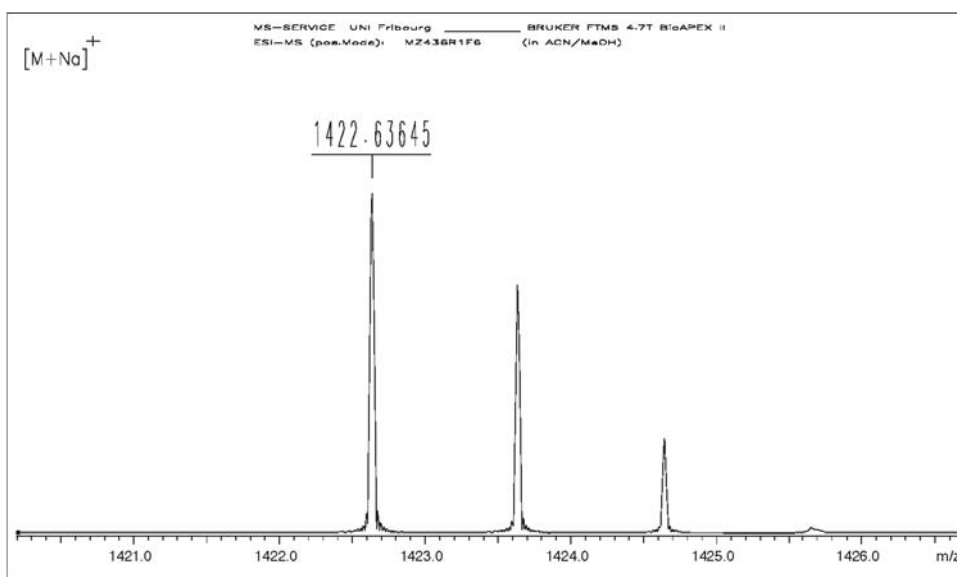


Figure S15. High-resolution mass spectrum (ESI+) of trimer **T-1**
 ([C₇₃H₉₇N₃O₂₄Na]⁺_{calc.} = 1422.63598).

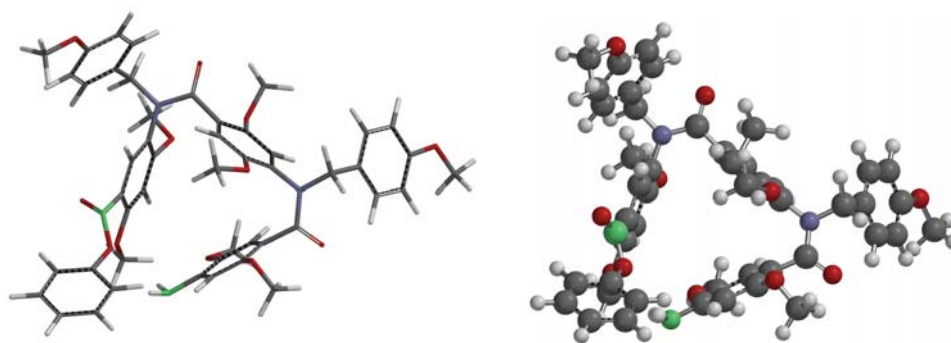


Figure S16. MMFF-AM-1-optimized structure of trimer **T-1** (*left*: tube model, *right*: ball and spoke model). TEG side chains are represented by methoxy groups and the reactive centers are highlighted in green.

Synthesis of the mono-PMB-protected trimer (T-2)

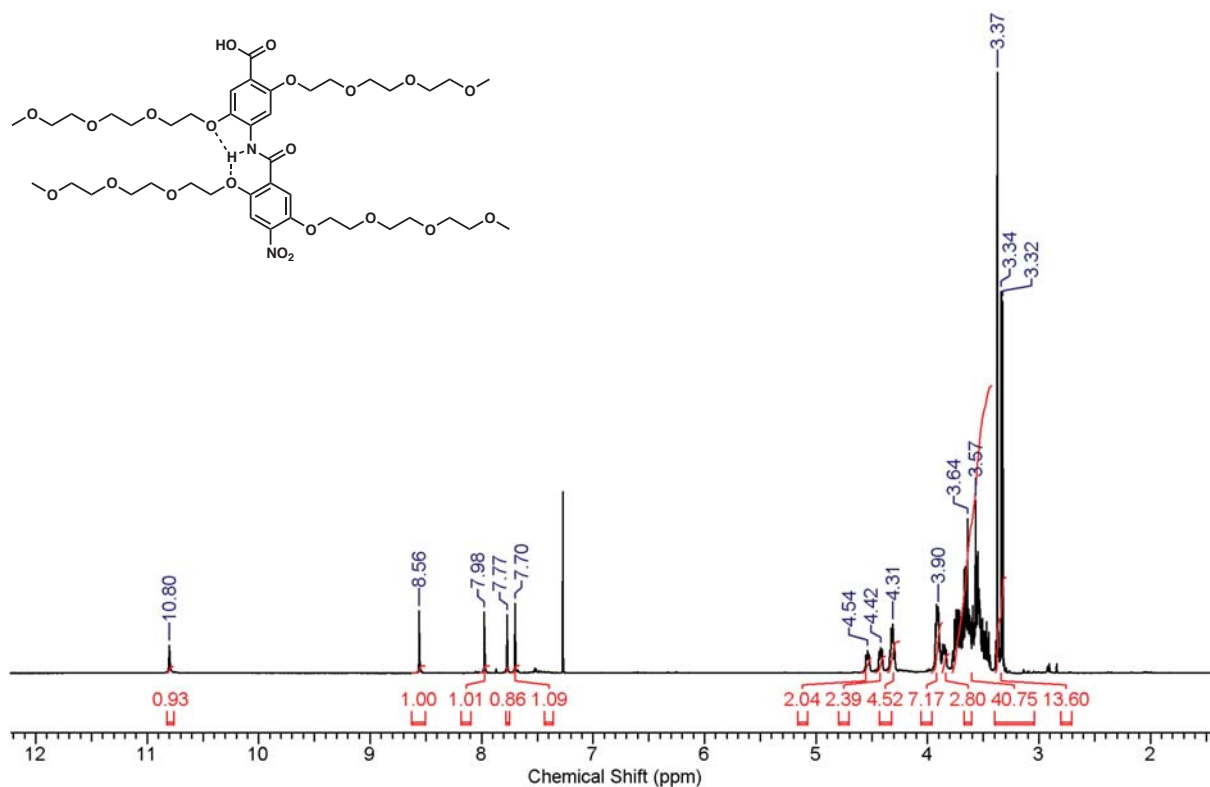


Figure S17. ¹H NMR spectrum (300 MHz, CDCl₃) of dimer **4**.

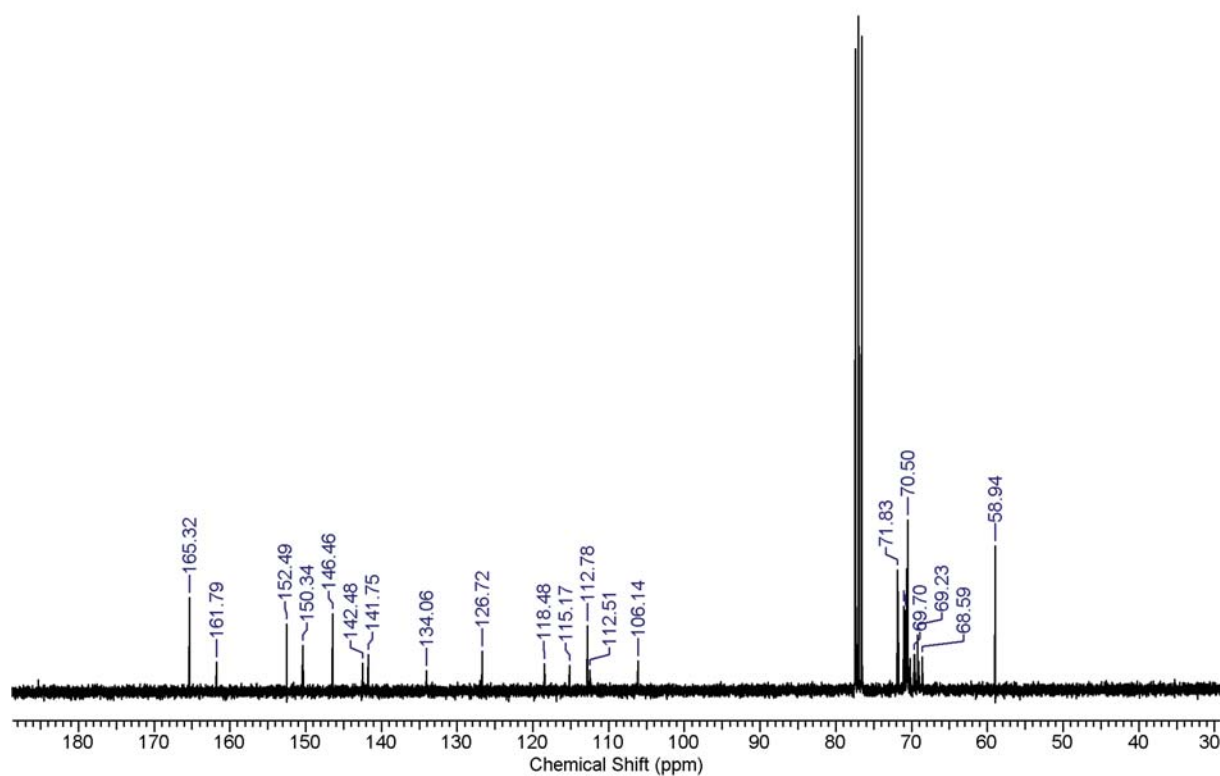


Figure S18. ¹³C NMR spectrum (75 MHz, CDCl₃) of dimer 4.

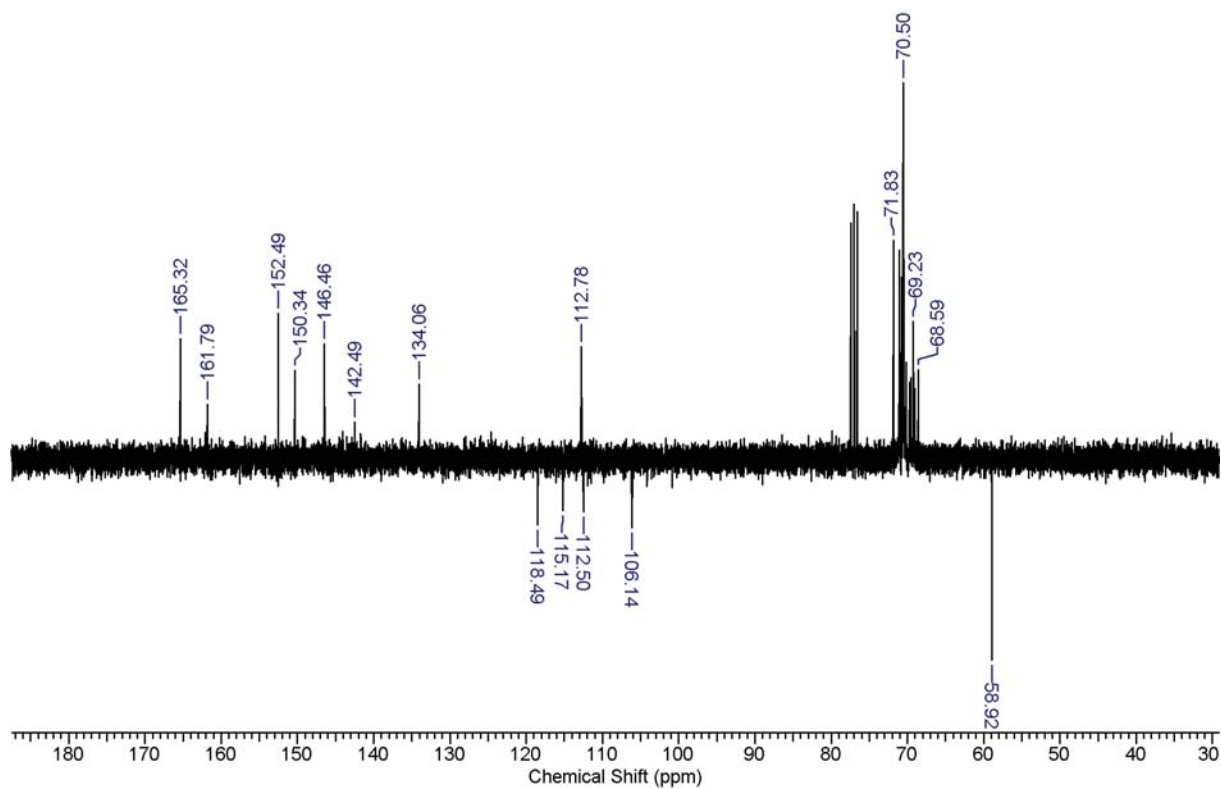


Figure S19. APT spectrum (75 MHz, CDCl₃) of dimer 4.

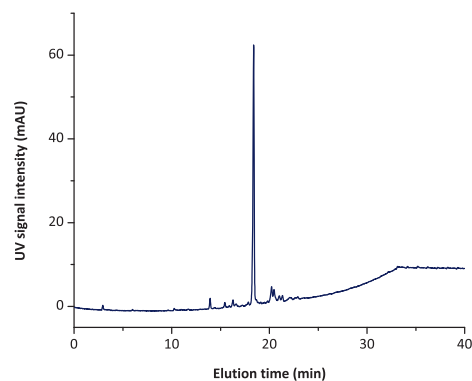
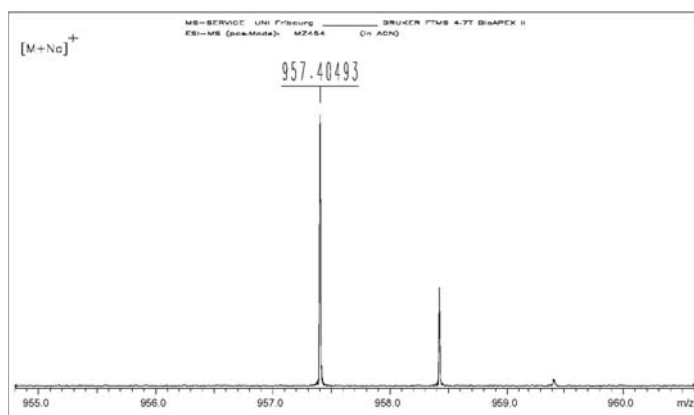


Figure S20. High-resolution mass spectrum (ESI+, $[\text{C}_{42}\text{H}_{66}\text{N}_2\text{O}_{21}\text{Na}]^+$ $_{\text{calc.}} = 957.40558$, *left*) and RP-HPLC elugram (*right*) of dimer **4**.

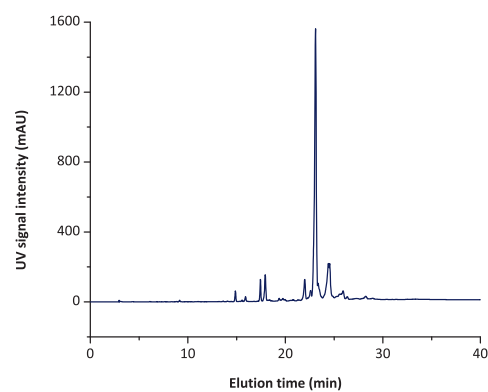
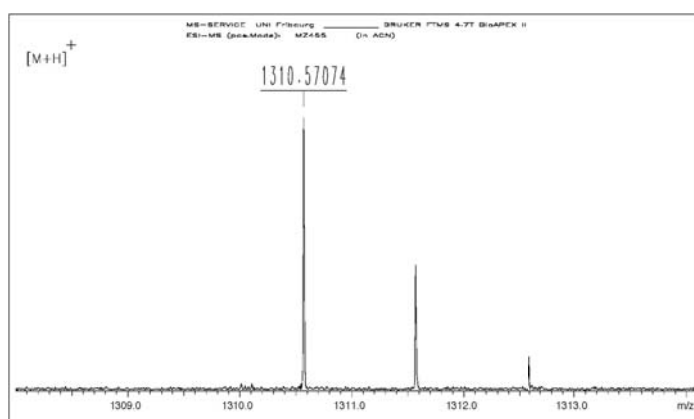


Figure S21. High-resolution mass spectrum (ESI+, $[\text{C}_{65}\text{H}_{88}\text{N}_3\text{O}_{25}]^+$ $_{\text{calc.}} = 1310.57070$, *left*) and RP-HPLC elugram (*right*) of trimer **5**.

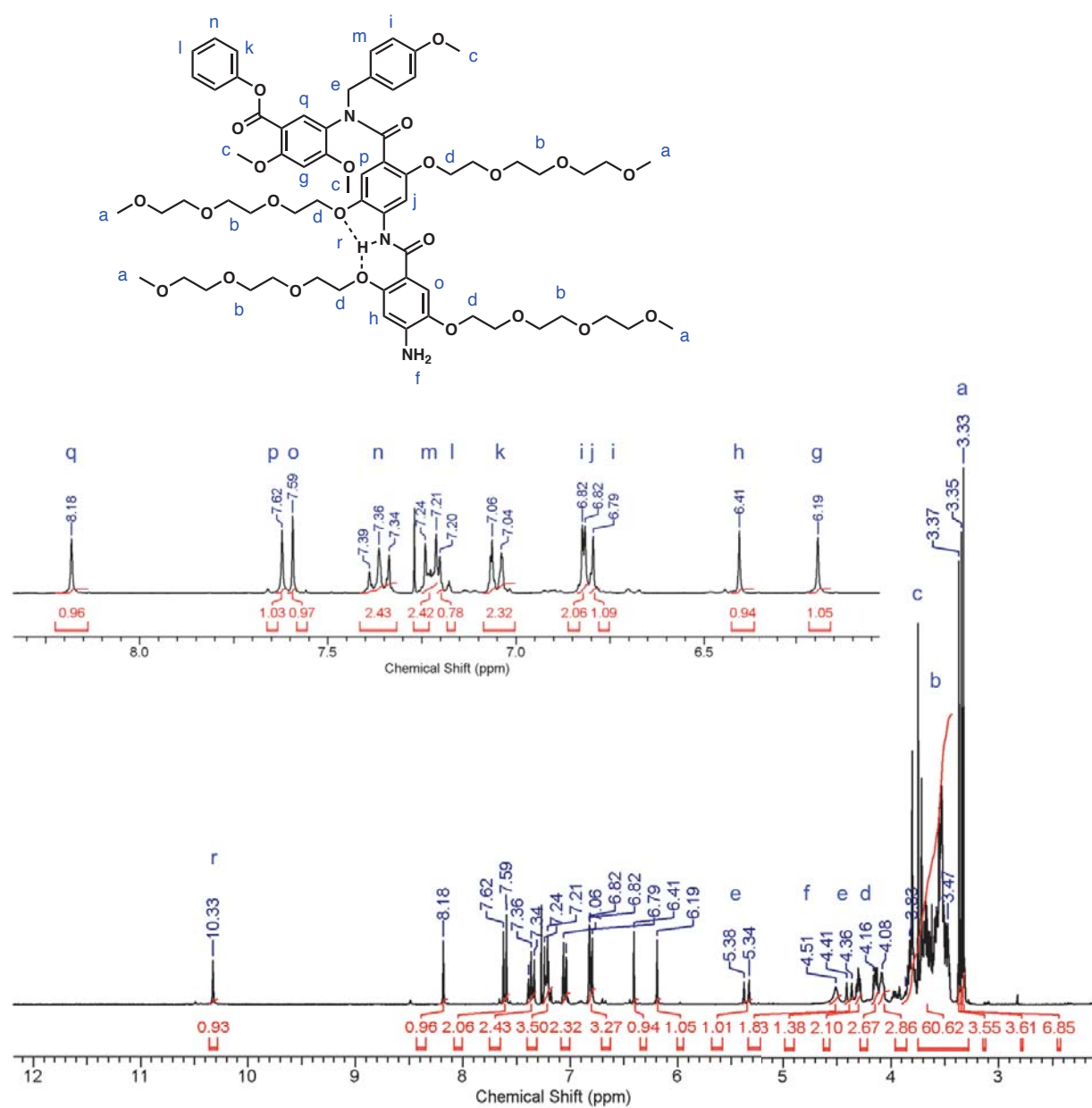


Figure S22. ^1H NMR spectrum (300 MHz, CDCl_3) of trimer T-2.

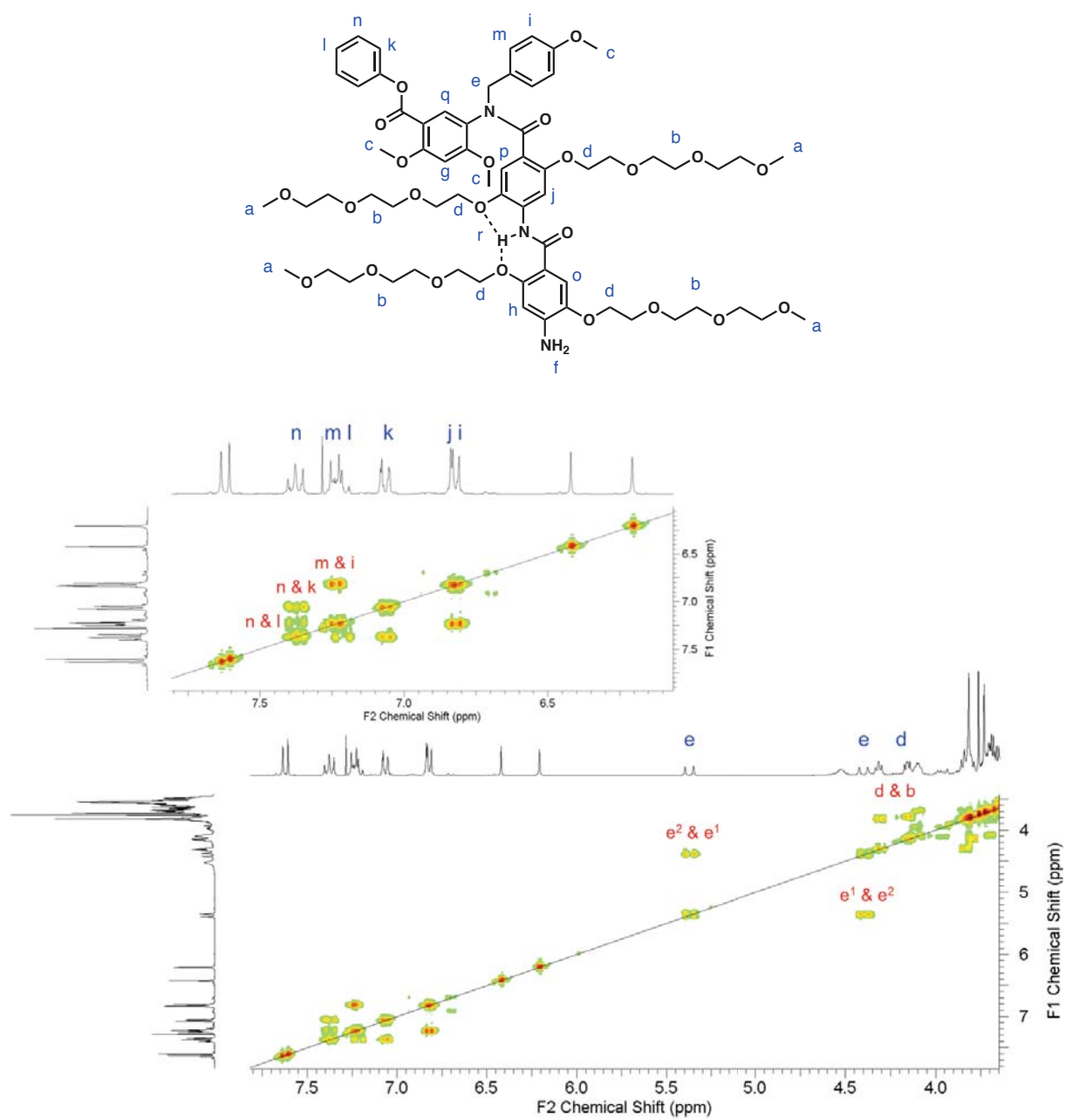


Figure S23. COSY spectrum (300 MHz, CDCl_3) of trimer **T-2** (sections).

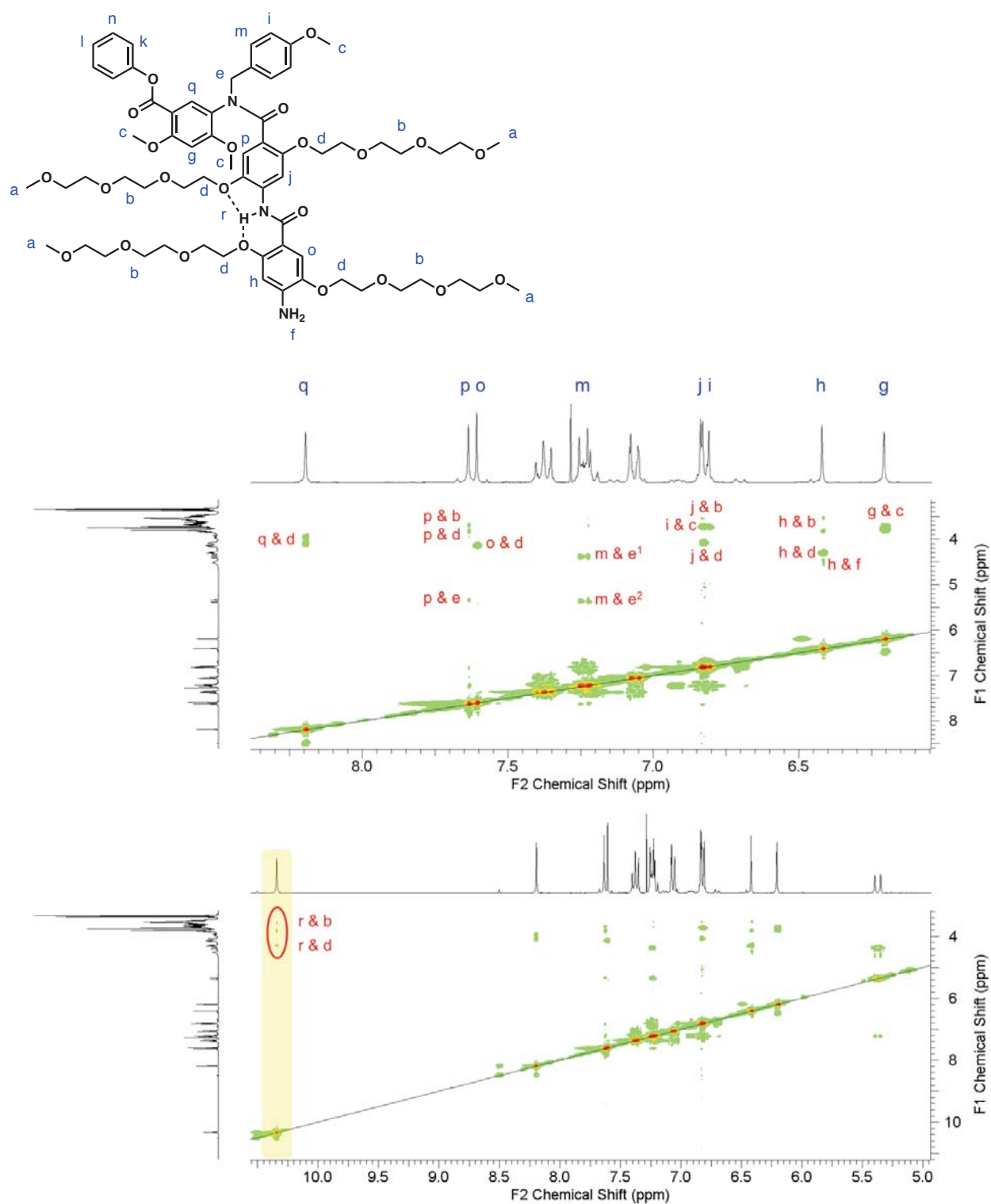


Figure S24. NOESY spectrum (300 MHz, CDCl₃) of trimer T-2 (sections).

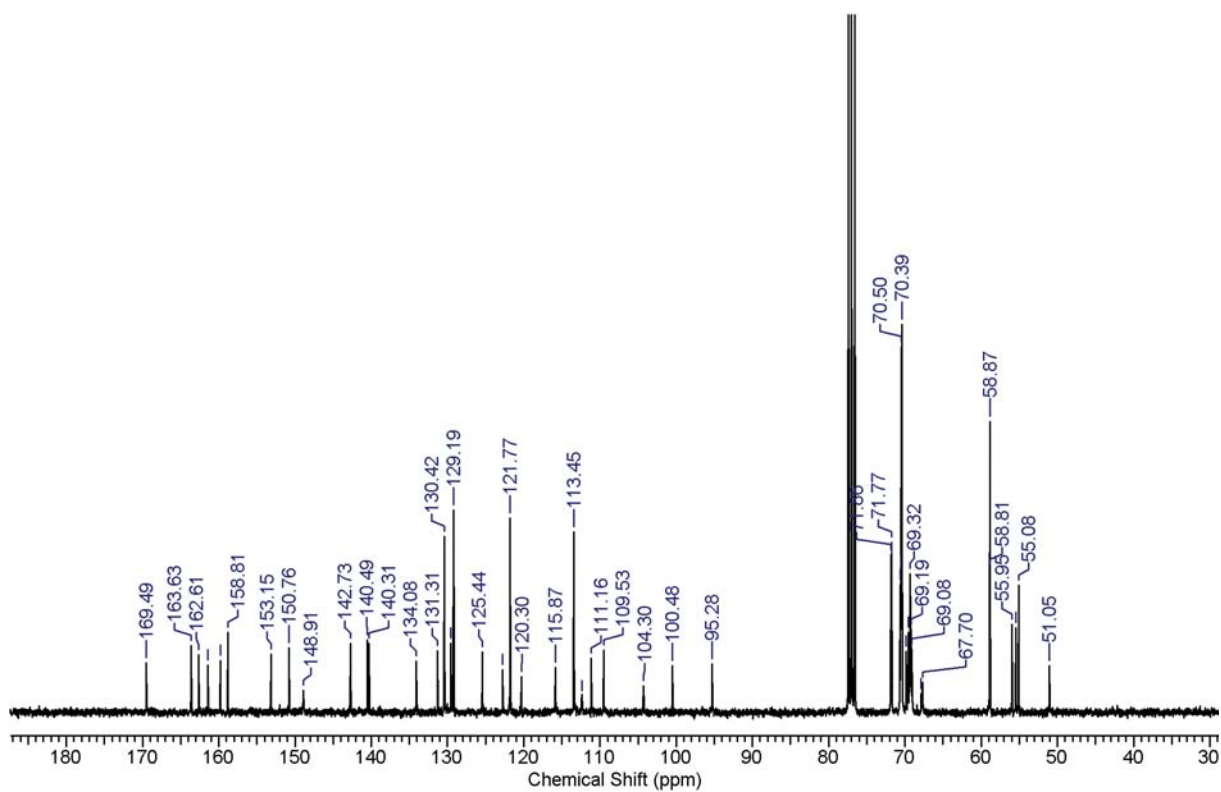


Figure S25. ¹³C NMR spectrum (75 MHz, CDCl₃) of trimer T-2.

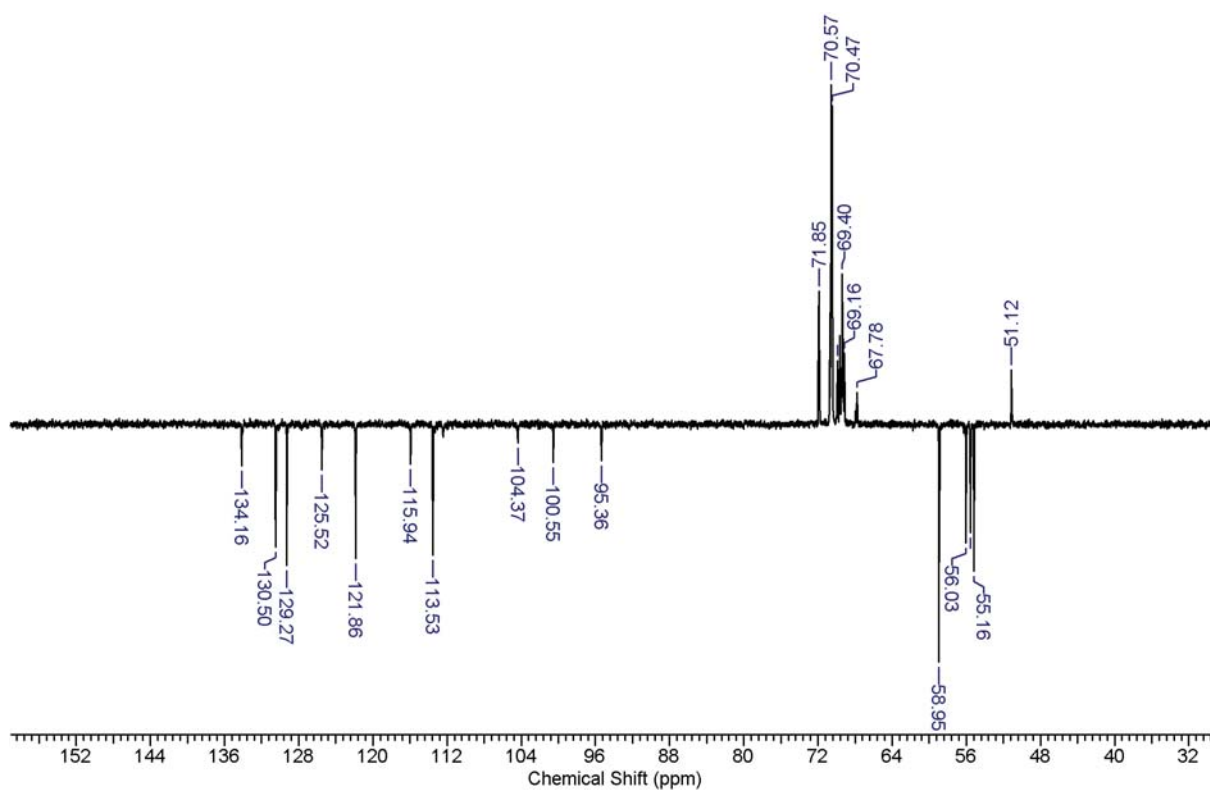


Figure S26. DEPT spectrum (75 MHz, CDCl₃) of trimer T-2.

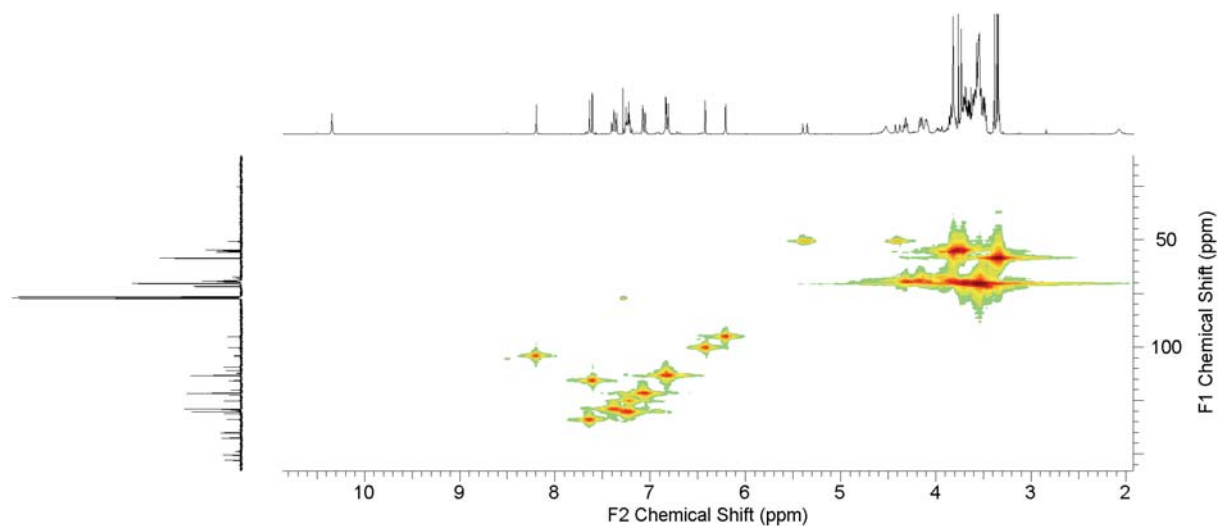


Figure S27. HMQC spectrum (300 MHz, 75 MHz, CDCl₃) of trimer **T-2**.

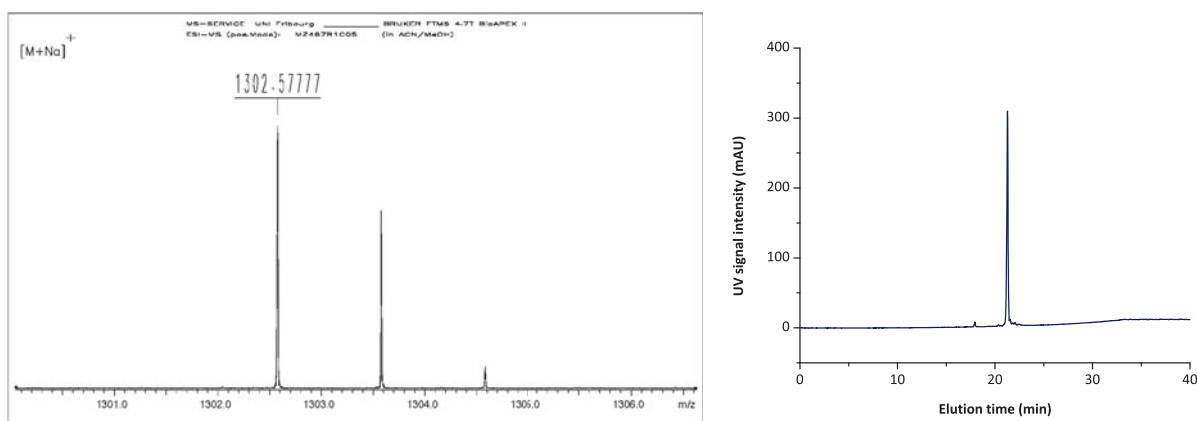


Figure S28. High-resolution mass spectrum (ESI+, $[\text{C}_{65}\text{H}_{89}\text{N}_3\text{O}_{23}\text{Na}]^+$ $_{\text{calc.}} = 1302.57846$, *left*) and RP-HPLC elugram (*right*) of trimer **T-2** after purification via recycling HPLC.

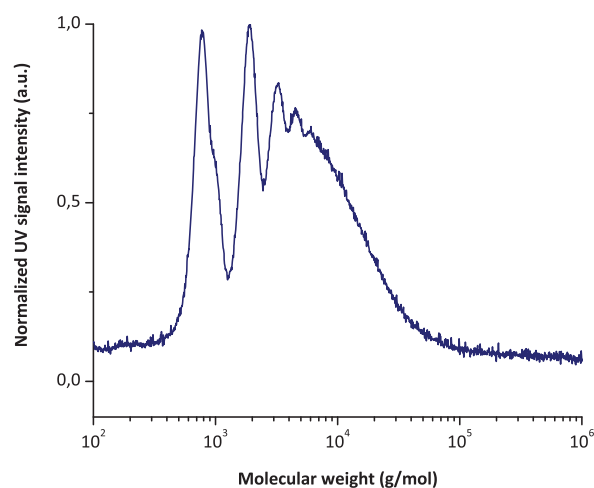


Figure S29. Molecular weight distribution of the second polycondensation of trimer **T-2** determined by CHCl_3 -GPC.

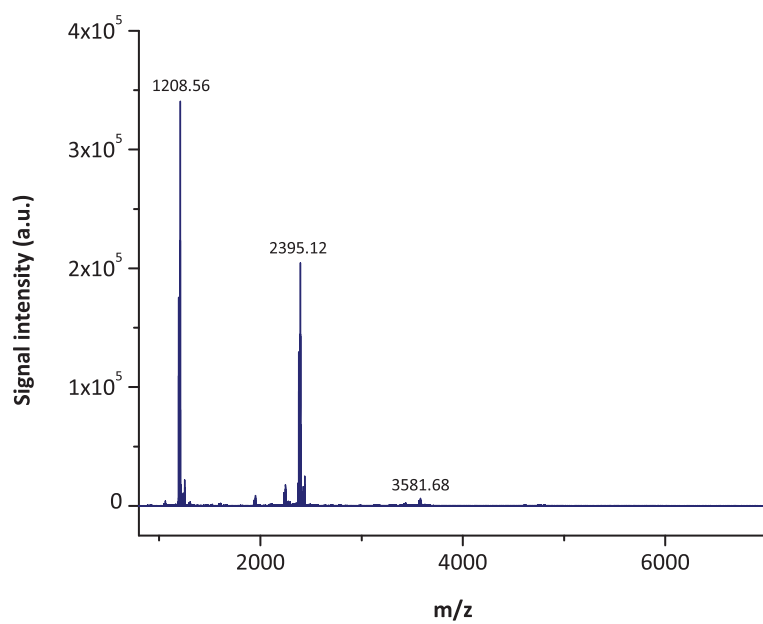


Figure S30. MALDI-ToF mass spectrum of the polymerization of trimer **T-2** (Na^+ -adducts).

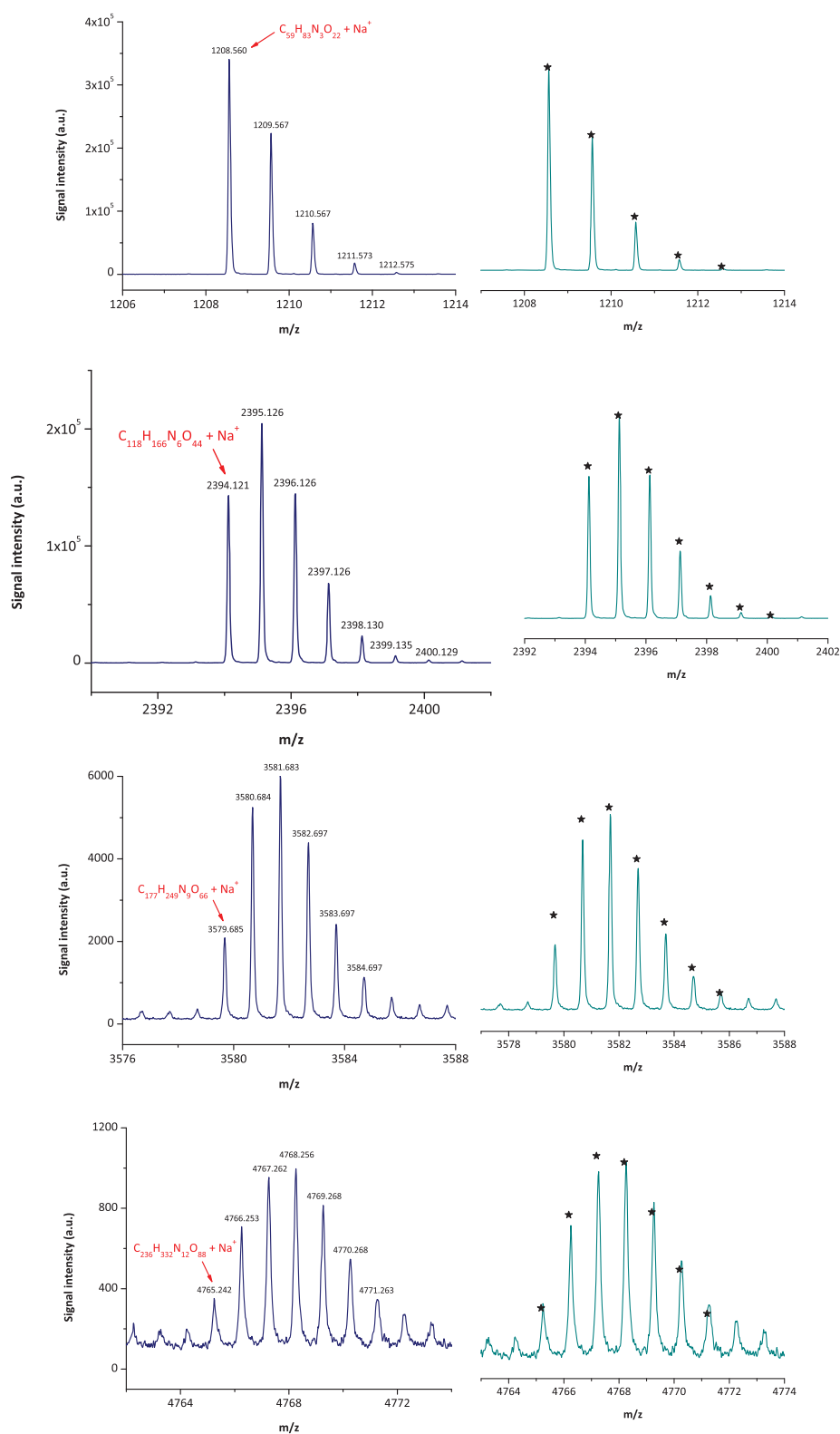
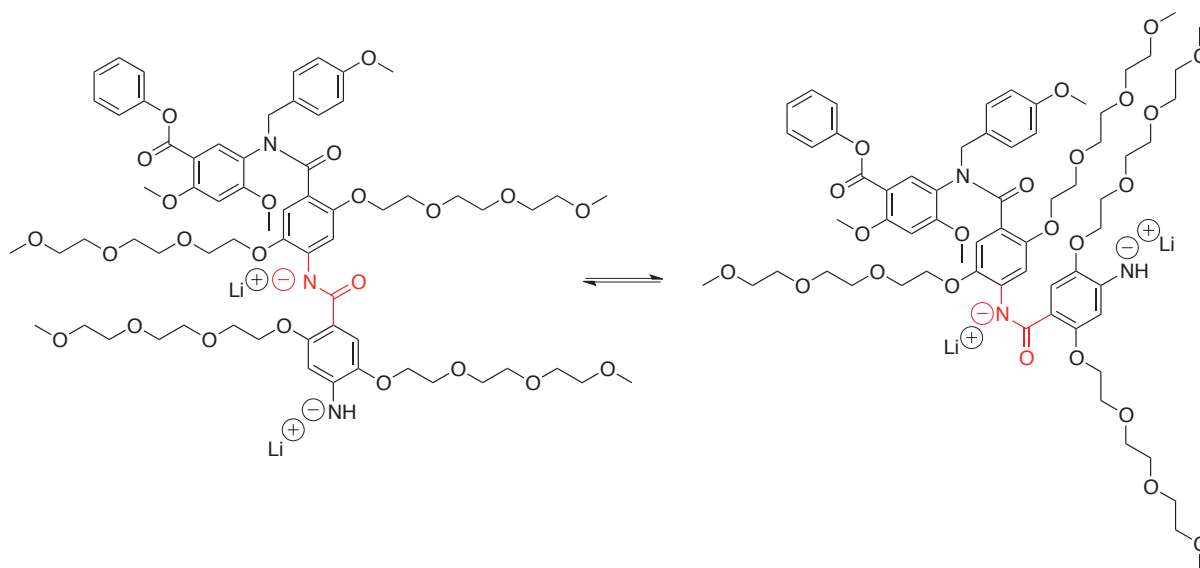


Figure S31. Sections of the MALDI-ToF mass spectrum of the cycles formed in polymerization **P-2**. From *top* to *bottom*: Cyclic trimer, cyclic hexamer, cyclic nonamer and cyclic dodecamer as Na-salts and the comparison of their isotope patterns (*green*) with the calculated one (*stars*).



Scheme S2. Equilibrium between the *trans*-(*Z*) and *cis*-(*E*)-conformation (both highlighted in *red*) of the deprotonated trimer **T-2** during polycondensation using LiHMDS.

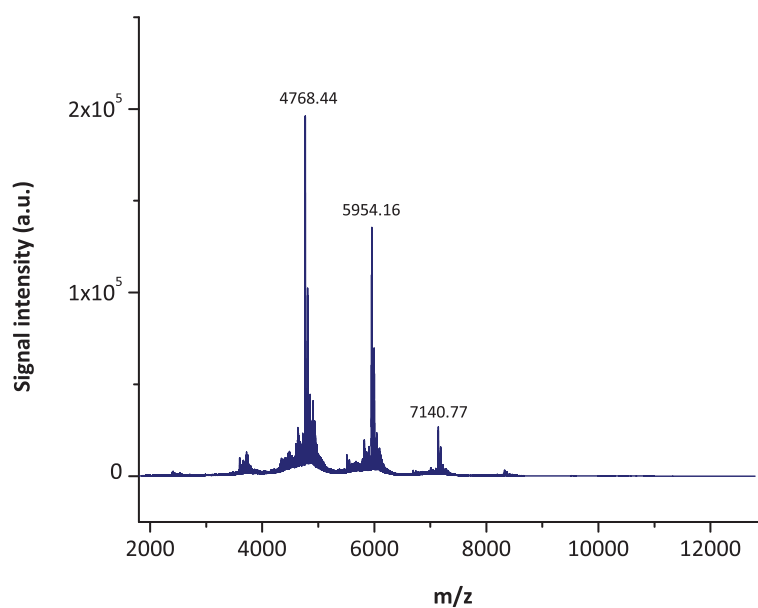


Figure S32. MALDI-ToF mass spectrum of polymer **P-2** (Li^+ -adducts) after separation via preparative GPC.

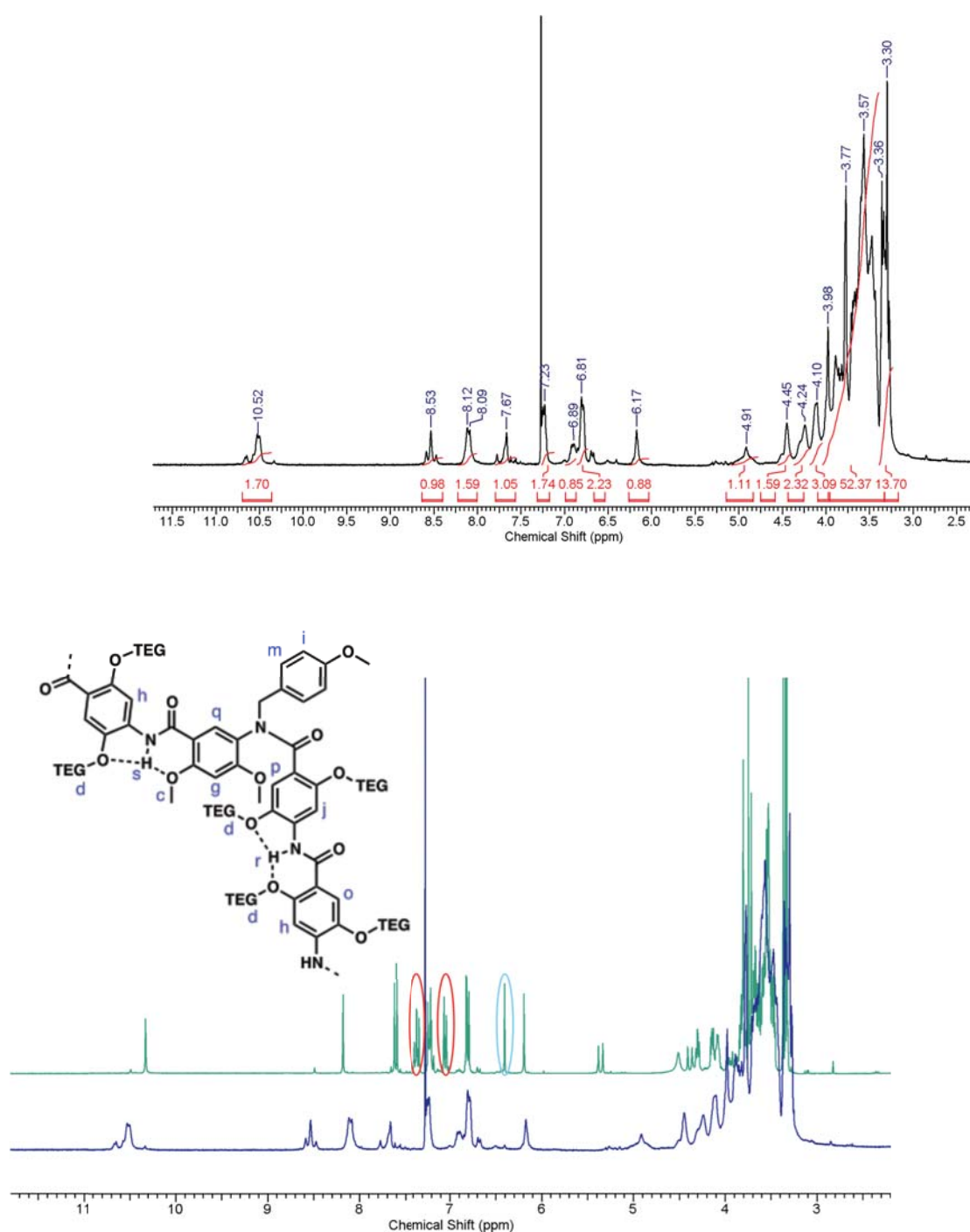


Figure S33. Top: ¹H NMR spectrum (300 MHz, CDCl₃) of polymer P-2 after separation via preparative GPC. Bottom: ¹H NMR spectra (300 MHz, CDCl₃) of the mono-PMB-protected trimer T-2 (green) and the corresponding N-protected polymer P-2 (blue). The disappearance of the peaks assigned to the phenyl ester (circled in red) and the shift of the proton h *ortho* to the N-terminal amine (circled in blue) verifies the successful amide bond formation.

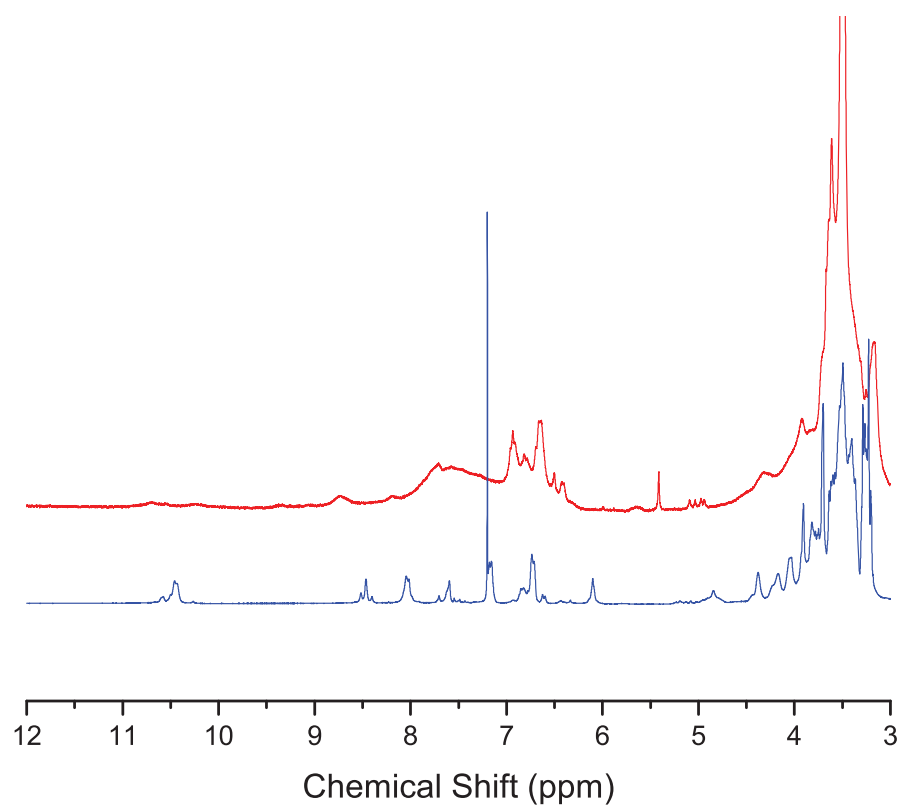


Figure S34. *Top:* ^1H NMR spectrum (300 MHz, THF-d_8) of polymer **H-1** (red)
Bottom: ^1H NMR spectra (300 MHz, CDCl_3) of the mono-PMB-protected polymer **P-2** (blue).